5th International Symposium on Multiphase Flow, Heat Mass Transfer and Energy Conversion
Xi'an, China, 3-6 July 2005

Numerical Analysis of Tissue Freezing in Cutaneous Cryosurgery Using Liquid Nitrogen Spray

Feng SUN[1], G.-X. WANG[1,*], Kristen M. KELLY[2], Guillermo AGUILAR[3]

1. Mechanical Engineering Department, The University of Akron, Akron, OH, 44325-3901, USA
2. Beckman Laser Institute, University of California, Irvine, CA 92612-1475, USA
3. Department of Mechanical Engineering, University of California Riverside, CA 92521, USA

Abstract Information on thermal history of skin tissue and iceball formation is critical for successful cutaneous cryosurgery. This paper presents a numerical analysis of tissue freezing during skin cancer treatment with liquid nitrogen (LN_2). A simplified mathematical model is constructed by including the bio-physical processes of the freezing tissues and quantifying LN_2 spray cooling with a convective heat transfer coefficient. Propagations of iceball fronts as well as lethal temperature isotherms are illustrated and quantitatively examined under various spray cooling conditions. The injury mechanisms of skin cells at different locations are also investigated based on corresponding thermal history and cooling rates during cryosurgery. These quantitative evaluations will be useful for pretreatment planning and optimization of LN_2 spray cryosurgical protocols.

1. Introduction

Medicinal use of tissue temperature manipulation is documented as early as 3500 B.C., when Egyptians used ice as a local anesthetic for wounds and other ailments [1]. However, cryosurgery using freezing to destroy undesirable tissues, was not developed until the 1850's when great progress was made on the development of low temperature physics, engineering and instrumentation. In 1845 and 1851, Dr. James Arnott, a British physician who first applied freezing for treatment of cancer, reported the use of a solution of crushed ice and sodium chloride to treat lesions in the breast and uterine cavity [2]. The development of the first cryosurgical probe in 1961 by Dr. Irving Cooper marked the beginning of modern cryosurgery, and in subsequent decades this technique was applied to gynecology, neurology, orthopedic surgery and dermatology [2].

Skin cancer is the most common malignancy in humans. Approximately 120,000 new cases are reported annually in the United States alone. It is conservatively estimated that the number of patients with pre-malignant skin tumors exceeds 5,000,000 [3]. The earliest application of cryosurgery to dermatology happened just before the pass of the 19th century, when Charles E. Tripler, a professor at Columbia University, devised a method to produce liquid air in quantity. A New York dermatologist, Dr. A. Campbell White, then used this cryogen to treat skin lesions [4]. The liquid air was later replaced by liquid nitrogen (LN_2), currently the most effective and most widely used cryogen.

Compared to alternative treatment modalities, cutaneous cryosurgery has many merits including: (i) brief treatment period; (ii) bloodless treatment field; (iii) minimal scarring and good cosmetic result; (iv) ease of performance; (v) high cure rate and (vi) low cost [4]. With these profound advantages, cutaneous cryosurgery has witnessed widespread acceptance in dermatological clinical practice for treatment of a wide range of skin lesions including actinic keratosis, warts, hypertrophic scars, keloids, mucoceles and solar lentigos [3,5].

Over the past decades, several techniques have been developed for cutaneous cryosurgery, including the swab and spray methods. The swab, essentially a cotton-tipped applicator saturated with LN_2, can be pointed, flat or round and is used to apply LN_2 directly onto the skin. Histological and thermal studies found that the freezing cannot destroy the cells located deeper than 1.5 mm from skin surface. This is inadequate for treatment of thick tumors [3]. Therefore, the LN_2 spray technique has become increasingly dominant in cutaneous cryosurgery [3,5]. This technique utilizes a canister with changeable nozzles which allow variation in the size of the LN_2 stream.

A successful cryosurgical process requires careful monitoring and evaluation of the freezing front. Otherwise, insufficient or excessive freezing may occur, and as a result, the recurrence of malignancies or destruction of healthy tissue may take place. Many researchers have been working to develop mathematical models to predict the extent and the thermal history of tissue freezing during cryosurgery. Trezek and Cooper [6,7] formulated one of the earliest models, which applied a bioheat transfer equation (i.e. Pennes bioheat equation) in unfrozen tissue, and obtained analytical solutions for steady-state as well as transient temperature fields. They even established a cryosurgical atlas to display the results of analytical and numerical computations such that a cryosurgeon can obtain a quantitative feel for the rate of iceball growth [8]. Comini and Del Giudice [9] later used the apparent heat

* Corresponding author. E-mail: gwang@uakron.edu

capacity method and finite element model to calculate the temperature fields produced by a hemisphere cryoprobe in actual tissue including the brain and angiomas. Rubinsky and Shitzer [10] optimized cryosurgery protocols by inverse mathematical techniques. Later, Rabin and Shitzer [11] developed more effective mathematical techniques for solving inverse-Stephen problems in non-ideal biological tissues. Using finite difference or finite element formulations of bioheat transfer equation, numerous computer simulations on tissue thermal distribution and freezing front evolution have been developed since the 1990s [12-19]. However, most research concentrated on the tissue freezing process induced by single or multiple cryoprobes, and few of them dealt with LN_2 spray.

Applying the two-dimensional finite volume formulation, the present study uses the apparent heat capacity method to simulate thermal history and phase change processes in human skin. The results can be used for clinical pretreatment planning and for design of optimal cryosurgery protocols.

2. Mathematical Model for Cutaneous Cryosurgery with LN2 Spray

During LN_2 cutaneous cryosurgery, the nozzle is positioned 1 to 1.5 cm from the skin surface and is aimed at the center of the target lesion, as schematically shown in Figure 1 [5]. Depending on the size, depth and location of the target lesion, different directional spray patterns can be chosen, for example, spot, paint, rotary and spiral sprays, among which, spot spray is most frequently used [5]. A cone shield is often used to confine the spray from splashing onto the surrounding healthy skin. A thermocouple needle placed percutaneously and positioned under the tumor may be used to monitor the temperature variation during the cryosurgery. When the spray gun is triggered, a combination of nitrogen gas and fine droplets of LN_2 impinge onto the skin surface and a LN_2 film may eventually form. Due to strong vaporization of the LN_2, the target skin tissue will be cooled down rapidly. When the temperature of the skin drops down to the tissue phase change temperature, the freezing process starts. An iceball develops through the epidermis into the dermis and encompasses the tumor. After the spray, the frozen tissue will experience a slow thawing process and the iceball will melt. Spray induced freezing and subsequent thawing are routinely described as the freeze-thaw cycle and will lead to cellular destruction and tissue injury by the following mechanisms [20]: dehydration and the resulting concentration of electrolytes; crystallization and the consequent rupture of cellular membranes; denaturation of the lipid-protein molecules within the cell membrane; thermal shock and vascular stasis.

It is generally accepted that two physical processes, heat transfer and phase change, dominate the tissue freeze-thaw cycle during cryosurgery. Delineated by phase change fronts, heat transfer domain in the tissue can generally be divided into three regions as schematically illustrated in Fig. 2, where regions I, II and III represent the frozen region, phase change region (i.e. mushy region) and unfrozen region, respectively. The phase change region (mushy zone) exists because biological tissues are non-ideal materials and the phase change process occurs over a relatively wide temperature range [11]. Being highly tissue type dependent, the upper limit of the range (T_{m1}) may vary between -0.5 ºC and -1 ºC, and the lower limit (T_{m2}) between -5 ºC and -10 ºC [11,19]. The phase change latent heat is liberated within this region. When the temperature drops lower than the phase change temperature (T_{m2}), the metabolism and blood perfusion are believed to cease. The unfrozen region is distinguished by two biophysical processes in living tissue: metabolism and blood perfusion. It is therefore customary to describe the heat transfer within unfrozen region by the classical Pennes bioheat equation [11].

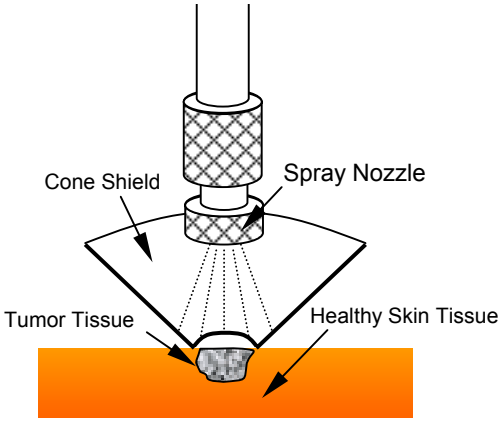

Fig. 1. Schematic of the cutaneous cryosurgery using LN_2 spray.

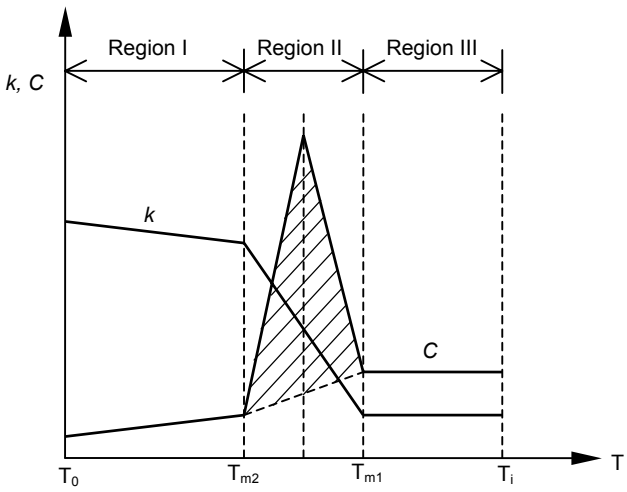

Fig. 2. Schematic presentation of the temperature-dependent thermal properties applied in the study.

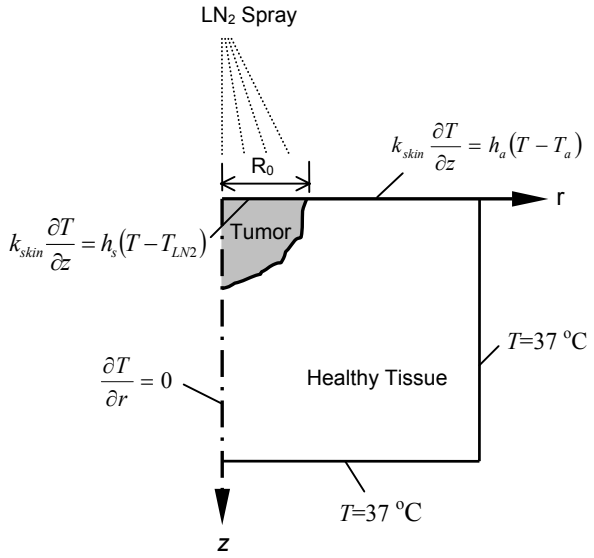

Fig. 3. Computation domain and boundary conditions.

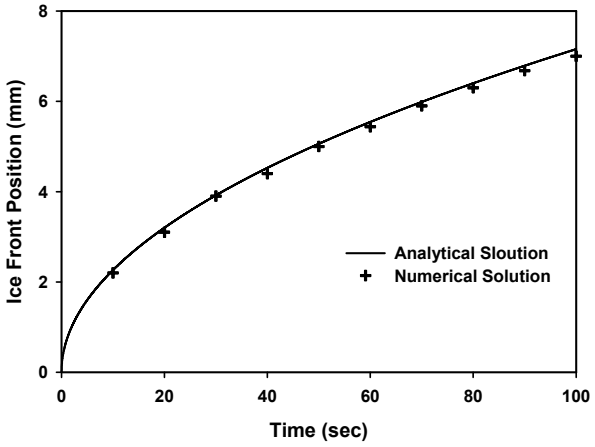

Fig. 4. Comparison of analytical and numerical solutions for ice front propagation.

Cutaneous cryosurgery is a complicated physical process involving not only complex bio-physical interaction as the tissues are cooled and frozen, but also complicated heat transfer mechanisms, including multiphase LN_2 spray convection and evaporation, heat exchange between the skin surface and LN_2, and latent heat release during phase change. The present study quantifies the effect of spray cooling on tissue and determines a thermal history of targeted cells. The process is significantly simplified by employing a series of assumptions:

(1) The LN_2 spray cone is assumed to be circular with uniform spray cooling within the impingement area. This allows simulation of heat transfer and phase change in the skin using an axisymmetric geometry system, as shown in Fig. 3. It is noted that, in reality, the heat transfer within the spray cone may vary in the radial direction [21].
(2) Skin tissue is treated as an isotropic medium with homogeneous properties and an initial uniform skin temperature of 37 ºC. The specific heat, the thermal conductivity, and the latent heat are estimated from the mass fraction of water within the tissue [9,19].
(3) Microscopic biophysical processes such as cell dehydration and intracellular ice formation (IIF) are not considered. Blood perfusion is considered to be negligible, but metabolic heat generation is included and assumed to be constant and uniform through the unfrozen region.
(4) The cancerous tissues and the healthy tissues are assumed to share identical thermal properties.
(5) The apparent specific heat of the solid/liquid mixture within the phase change range is assumed to vary linearly from the solidus temperature to liquidus temperature.

Based on the above assumptions, the mathematical equations for modeling the heat transfer in each of the three regions can be written as:

$$\rho_\zeta C_\zeta \frac{\partial T}{\partial t} = \frac{1}{r}\frac{\partial}{\partial r}\left(k_\zeta r \frac{\partial T}{\partial r}\right) + \frac{\partial}{\partial z}\left(k_\zeta \frac{\partial T}{\partial z}\right) + Q_m \qquad (1)$$

with $$Q_m = \begin{cases} 1240\, W/m^3 \text{ [8]} & T > -0.5°C \\ 0 & T \le -0.5°C \end{cases}$$

where the subscript ζ denotes the frozen (I), phase change (II) and unfrozen regions (III), respectively.

The computational domain and boundary conditions are schematically illustrated in Fig. 3, where the shaded area represents the skin tumor. In Fig. 3, it is assumed that the spray cone radius impacting on the skin surface, R_0 = 2.5 mm, is the same as the pathologic radius of the tumor at the skin surface. LN_2 spray cooling is represented by a convective heat transfer coefficient, h_s, while outside of the spray cone, heat is supplied to the skin surface from the room air with a much smaller convective heat transfer coefficient, h_a:

$$k_{skin}\left.\frac{\partial T}{\partial z}\right|_{z=0} = \begin{cases} h_s\left[T(r,0,t) - T_{LN2}\right] & 0 \le r \le R_0 \\ h_a\left[T(r,0,t) - T_a\right] & R_0 < r \end{cases} \qquad (2)$$

where k_{skin} is the skin thermal conductivity, T_{LN2} is the temperature of LN_2 at the skin surface, taken as -196 ºC, the saturated temperature of LN_2 at atmospheric pressure, and T_a is the room air temperature. All other boundaries are set to be the tissue temperature (e.g., T = 37 °C).

The commercial CFD software package, FLUENT (Fluent, New Hampshire), is used to solve the above mathematical problems. An apparent heat capacity method is used to treat the phase change process. The numerical method is first validated by solving a 1-D water-ice phase change process in half-space. The water at an initial uniform temperature, T_i = 20 ºC, is confined to a semi-infinite space $x > 0$. At time $t = 0$, the boundary surface at $x = 0$ is lowered to a temperature, T_0 = -50 ºC, and maintained. As such, solidification starts at the surface $x = 0$ and the ice front moves in the positive x direction. The exact solution for ice front location x

versus time t is given by Ozisik [22] as follows:

$$x(t) = 2\lambda(\alpha_s t)^{1/2} \tag{3}$$

where α_s is the thermal diffusivity of ice and λ is the root of the following transcendental equation:

$$\frac{e^{-\lambda^2}}{erf(\lambda)} + \frac{k_l}{k_s}\left(\frac{\alpha_s}{\alpha_l}\right)^{1/2} \frac{T_m - T_i}{T_m - T_0} \frac{e^{-\lambda^2(\alpha_s/\alpha_l)}}{erfc\left[\lambda(\alpha_s/\alpha_l)^{1/2}\right]} = \frac{\lambda L\sqrt{\pi}}{C_s(T_m - T_0)} \tag{4}$$

Once λ is found, the ice front propagation can be plotted using Eq. (3). Figure 4 shows examples of numerical results calculated using FLUENT as compared to the above analytical solution. As one can see, the ice front propagation obtained by numerical solution agrees well with the analytical solution. The small difference results because the apparent heat capacity method has to assign a small "mushy" region even for a pure material.

3. Thermal Properties of Skin Tissues

Smith *et al*. [23] noted that the predicted thermal history of an iceball is strongly affected by temperature-dependent thermal properties. The present study estimates the thermal properties for frozen tissue by assuming that the non-water portion conducts a negligible amount of heat. Thermal properties for unfrozen and frozen skin tissue were calculated (Table 1) taking into consideration that human skin tissue consists of 65% water [24], and the temperature dependence of the thermal properties of water is taken from Alexiades and Solomon [25]. The upper limit temperature (liquidus) of the phase change region, T_{m1} = -0.5 ºC, the initial freezing point of plasma [9]; and the lower limit temperature (solidus), T_{m2} = -10 ºC, are obtained from Hoffman and Bischof's work [19]. The metabolic heat generation source term and the temperature dependence of the thermal properties are implemented in FLUENT by user defined functions (UDF).

Table 1. Thermal properties of skin tissue used in the model.

k_u (W/m K)	0.39
k_f (W/m K)	$1.46+3.88\times10^{-3}\cdot(273-T)^{1.156}$
C_u (J/Kg K)	2721
C_f (J/Kg K)	89.7+5.04T
ρ (Kg/m^3)	1116
L (J/Kg)	217100
Q_m (W/m^3)	1240
T_{m1} (ºC)	-0.5
T_{m2} (ºC)	-10

4. Results and Discussions

In our model, the cooling condition of the LN_2 spray is simplified by an average heat transfer coefficient, h_s, which may vary depending on tank pressure, nozzle size, and spray distance [26]. h_s may also vary with time as the skin surface temperature decreases. Little information is available in the literature on LN_2 spray under the present configuration. Therefore, a range of values of h_s is employed in this study, varying from 10^4 to 10^6 W/m^2 K, to examine the effect of h_s on iceball formation.

During cryosurgery, the LN_2 spray duration is also an important parameter. The effect of spray duration is therefore investigated. For any give value of h_s and spray duration, the iceball formation, represented by the propagation of the liquidus and solidus isotherms, are examined quantitatively. In addition, the thermal history of tissues, the cooling rate and the lethal temperature isotherm propagation are also examined in a quantitative manner.

Isotherms Evolution

A typical frozen front propagation for $h_s = 10^6$ W/m^2 K is shown in Fig. 5 by the isotherms evolution (T_{m1} and T_{m2} for unfrozen/mushy zone interface and frozen/mushy zone interface, respectively). As one can see, once the LN_2 spray impinges on the skin surface, the isotherms start to propagate along both axial and radial directions,

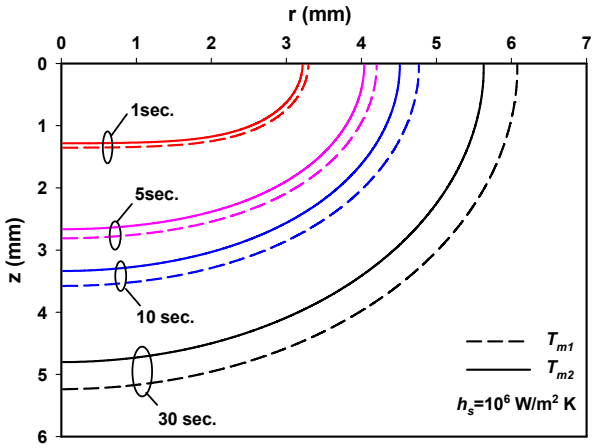

Fig. 5. Frozen front propagation (h_s=10^6 W/m^2 K). T_{m1} = unfrozen/mushy zone interface; T_{m2} = frozen/mushy zone interface

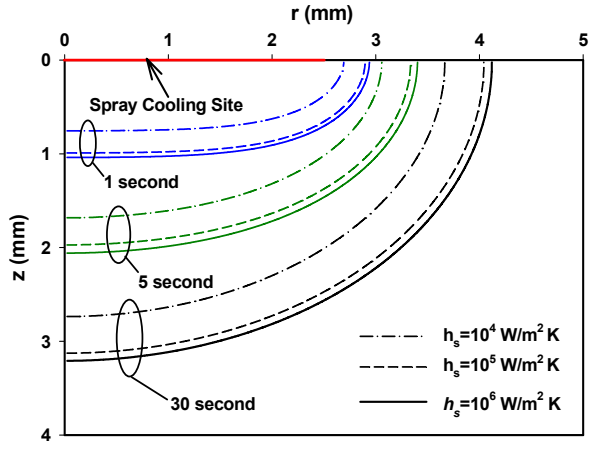

Fig. 6. Propagation of lethal temperature (-50 °C) isotherms.

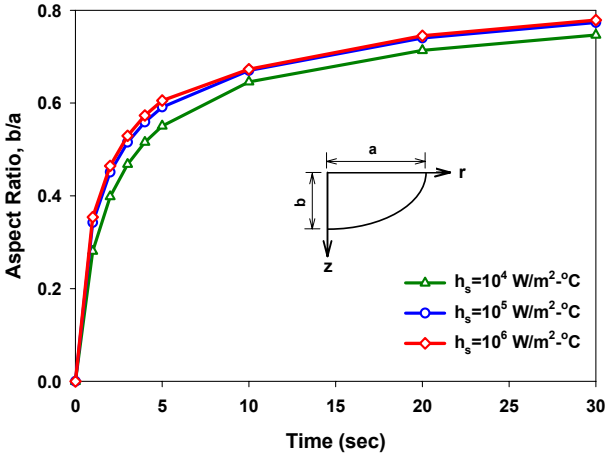

Fig. 7. Variation of the aspect ratio of depth (*b*) to lateral distance (*a*) of the lethal temperature (-50 °C) isotherms from the center of spray.

but propagation rate along the axial direction (i.e. the direction penetrating into the skin) occurs faster than that in the radial direction (i.e. parallel to the skin surface). As a result, if the duration of the spray lasts long enough, the shape of the frozen volume evolves from an initial half flat ellipse to an almost half sphere. Ideally, cryosurgery will create an iceball encompassing the whole tumor while being minimally invasive to the surrounding healthy tissue. Figure 5 indicates that a cryosurgeon should be able to manipulate iceball evolution by controlling spray duration.

Another critical thermal parameter in cryosurgical quantitative analysis is the lethal temperature. Freezing a tumor to or lower than the lethal temperature will completely destroy the tumor. Numerous publications have shown that lethal temperatures are highly cell and tissue type dependent, ranging from -10 ºC for MBT-2 bladder carcinoma [27,28] to -50 ºC in healthy skin tissue [29]. –50 ºC is now widely accepted as the lethal temperature for malignant skin tumors by dermatologists [29,30,31]. Figure 6 shows the propagation of lethal temperature isotherms for various values of h_s and reveals that the lethal temperature isotherms propagate, similar to the tissue phase change fronts, non-homogeneously along different directions (more quickly in axial as compared to in lateral). This phenomenon can be further elucidated by Fig. 7, where the aspect ratio, *b*/*a*, is introduced to show the evolution of the lethal temperature isotherms, where *b* is the distance of the isotherm from the spray center in the z direction and *a* is the distance of the same isotherm from the center of the skin surface as defined in the insert in Fig. 7.

In clinical practice, the relative importance of the phase change temperatures and the lethal temperature depends mainly on the type of target tissue. For malignant tumors, one has to make sure that all the cancerous cells are destroyed entirely by freezing, and lethal temperature isotherms should be utilized, choosing a relatively wide margin beyond the pathologic border

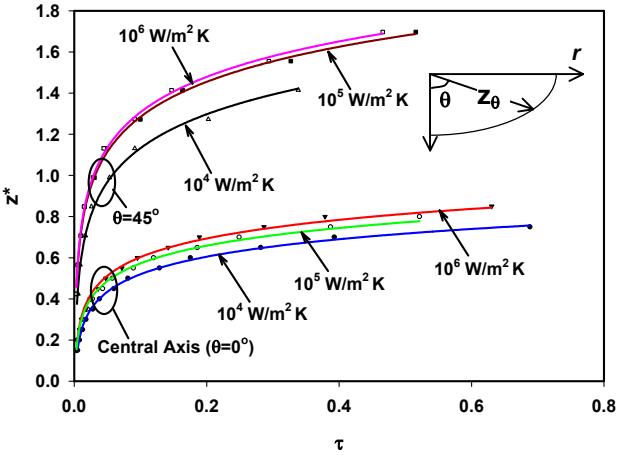

(a)

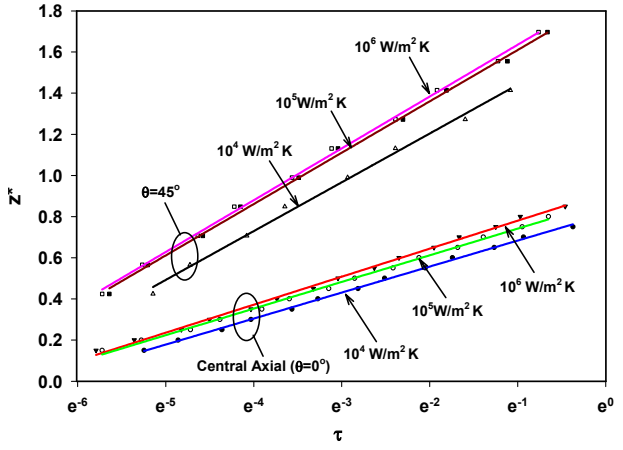

(b)

Fig. 8. Propagation of lethal isotherms along different directions: (a) τ in linear scale; (b) τ in logarithmic scale.

[5]. On the other hand, if the target is a benign lesion, the cryosurgeon wants to limit freeze injury of healthy tissue. In this case, a much smaller margin or even no margin is desired, and phase change temperature isotherms can be used to optimize the cryosurgical protocol.

Penetration Depth and Time

To ascertain whether the target tissue, which is geometrically irregular in most cases, is entirely enclosed by the lethal temperature isotherm, one needs to know the time penetration depth of the lethal temperature along different directions. This is presented in Fig. 8, where the dimensionless penetration depth z^* and the dimensionless time τ are defined as follows:

$$z^* = \frac{z_\theta}{R_0}, \quad \tau = \frac{\overline{\alpha} \cdot t}{R_0^{\,2}} \tag{5}$$

In the definition, z_θ is the distance between the center of the spray on the surface and the lethal temperature

isotherm along the direction forming an angle θ with the central axis (see the insert in Fig. 8a), R_0 is the radius of the spray cooling area, and $\bar{\alpha}$ is the temperature weighted thermal diffusivity, calculated as follows:

$$\bar{\alpha} = \frac{\bar{k}}{\rho \cdot \bar{\bar{C}}} \tag{6}$$

where $\bar{\varphi} = \dfrac{\int_{77}^{310} \varphi(t)dt}{310-77}$ with $\varphi = k$ or C. The temperature dependences of k_f and C_f are listed in Table 1.

Fig. 8a demonstrates that the lethal isotherm propagates fast at the beginning of the spray and then slows down gradually as the cryosurgery proceeds. The change of z^* with respect to the dimensionless time τ shows a natural logarithmic form and can be fitted by the following equation:

$$z^* = m + n \cdot \ln \tau \tag{7}$$

where the regression constants of m and n correspond, respectively, to the intercept and slope of the curves shown in Fig. 8b and list in Table 2.

Table 2. Regression constants, m and n, for lethal temperature isotherm propagation along different directions.

θ	h_s (W/m^2 K)	m	N
0°	10^4	0.8101	0.1264
	10^5	0.8712	0.1295
	10^6	0.9165	0.1362
45°	10^4	1.679	0.2373
	10^5	1.860	0.2497
	10^6	1.888	0.2520

The regression constants, m and n, are functions of the convective heat transfer coefficient, h_s, when h_s is smaller than 10^5 W/m^2 K. Further increasing h_s to 10^6 W/m^2 K, however does not show significant change in z^*. Since the depth of the lethal temperature is critical for destruction of cancer cells, Eq. (7) could be useful for quantitative evaluation of freezing effect in early planning.

Figure 8a also shows that progression rate of the lethal isotherm decreases with time. This can be understood by remembering that the isotherm area increases as the lethal isotherm penetrates deeper into the skin. In addition, heat conduction resistance within frozen tissue becomes a dominating factor in the heat removal process, and meanwhile, there is a decrease in the convective heat transfer between the skin and sprayed LN_2. When the spray initiates, a big temperature difference between the skin surface (37 ºC) and LN_2 (-196 ºC) exists. Such a great temperature difference leads to an initial large heat flux which, however, drops quickly as the skin surface approaches the LN_2 temperature. The rapid drop of skin temperature near the cutaneous surface can be observed clearly in Fig. 9, which shows temperature curves of tissue beneath the cooling site center as a function of depth. As one can see, the temperature at z = 1 mm drops down to almost the LN_2 temperature within a few seconds, and remains at the temperature till the spray ends. Therefore, during the majority of the cryosurgery procedure, there is a small temperature difference between the surface temperature and the LN_2 temperature. As such, heat removal from the skin is strongly dependent on agitation of the deposited LN_2 film on the skin surface, which is represented in this study by the heat transfer coefficient, h_s.

Cooling Curves and Cooling Rates

Cellular injury requires more than achievement of the lethal temperature. Equally important is the thermal history of a cell, including the cooling rate and hold time, the duration a cell is maintained at or lower than the lethal temperature [28].

Cooling rate plays a significant role in determining cell injury in cryosurgery. It is well accepted now that two biophysical events may cause cell injury and death during freezing: cell dehydration by water transport across the cell membrane (i.e. solute or solution effects), and IIF. When cells together with their extracellular matrix are cooled below the phase change temperature, ice forms first extracellularly, and the solute concentration outside the cell begins to increase. If the cooling rate is low, the intracellular water has sufficient time to diffuse through the plasma membrane to balance the osmotic pressure difference between the intracellular and extracellular spaces. As a result, cells become dehydrated and intracellular solutes are highly concentrated. This will result in damage to cellular proteins and enzymatic systems, and cell plasma membranes can be destabilized [32]. On the other hand, if the cooling rate is high, intracellular water has little time to leave the cell, ice nucleates inside the cell and IIF occurs. IIF causes injury to cell membranes and is thought to damage cellular organelles and cytoskeletons [32].

Figure 9 presents the typical thermal history (cooling curves) for tissue at several different locations along the

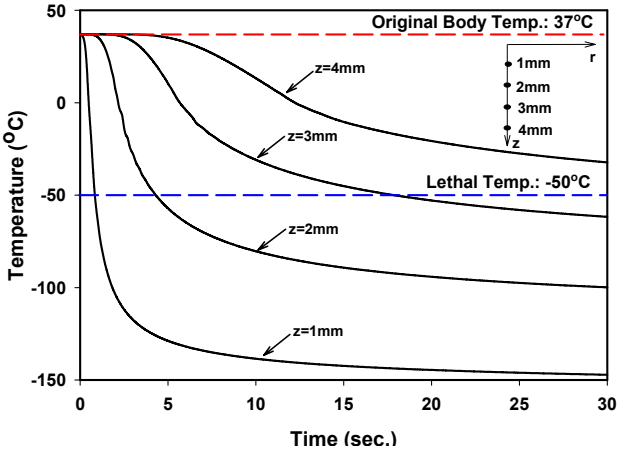

Fig. 9. Temperature curves of tissue beneath the cooling site center as a function of depth (h_s=10^6 W/m^2 K).

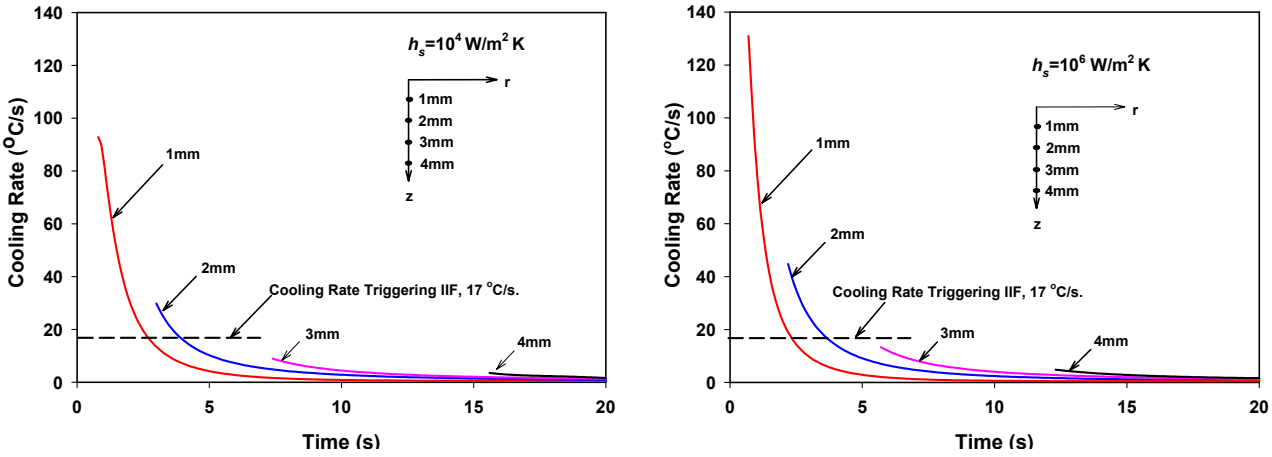

(a) (b)

Fig. 10. Cooling rates underneath the skin surface. (a) h_s=10^4 W/m^2 K; (b) h_s=10^6 W/m^2 K.

central axis as measured from the skin surface: z = 1, 2, 3 and 4 mm. A 30-second continuous spray, commonly used in clinical practice [5], is considered and the convective heat transfer coefficient is fixed at 10^6 W/m^2 K, a fairly high value.

It is evident that it takes less time for the skin surface to reach the lethal temperature as compared to deeper regions. Therefore, while tissue close to the skin surface cools rapidly leading to IIF, deeper layers experience much slow cooling rates, allowing equilibration of solutes between the intra and extracellular compartments and resultant cellular dehydration. Furthermore, at the most superficial layers, as intracellular ice remains below phase change temperature for a longer period, recrystallization of the ice (ice crystals fuse to form larger crystals to decrease the surface area and minimize free energy) may occur. This would result in disruption of cell membrane or organelles [28]. Figure 9 also shows that the tissue temperature 4 mm beneath the skin surface has not dropped to the lethal temperature after 30 seconds. As a result, some cells at this position are likely to recover viability after the freeze-thaw cycle and, "edge recurrence" may occur.

Figure 9 demonstrates that tissue cooling rate is highly dependent on time and tissue location. It is therefore necessary to discuss cooling rate as a function of time and space, as shown in Figs. 10a and 10b. The cooling rate curves in Fig. 10 start from the moment when the temperatures drop to the phase change temperature T_{m1}. For convenience, it is assumed that IIF occurs when the cooling rate exceeds 1000 ºC/min (≈17 ºC/s), a calculated result from Mazur *et al* [33]. When the tissue temperature drops to T_{m1}, the cooling rates at 1 mm and 2 mm beneath the skin surface exceed 17 ºC/s, while those at 3 mm and 4 mm do not. One can therefore expect that the IIF region will occur in cells 2 mm beneath the skin surface or less while cells located at 3 mm and deeper are more likely to witness extracellular ice formation and, therefore, suffer cellular dehydration.

5. Conclusions

A mathematical model has been developed for LN_2 cutaneous cryosurgery. Freezing of skin tissue is assumed to take place over a temperature range from -0.5 °C to -10 °C. Blood perfusion is neglected in all cases, while metabolism is considered in unfrozen regions. Heat transfer between the skin and the sprayed LN_2 is simplified by a convective heat transfer coefficient, h_s, with the LN_2 film on the skin surface assumed to be as saturation temperature at the atmospheric pressure. The model allows detailed evaluation of iceball formation during cutaneous cryosurgery and propagation of lethal temperature isotherms. Iceball fronts and lethal temperature isotherms are spatially inhomogeneous, progressing rapidly axially and more slowly laterally. Examination of the thermal history shows that targeted tissues at different depths will experience varied injury mechanisms. For example, along the central axis, rapid LN_2 cooling will induce IIF for cells approximately 2mm from the skin surface or less, while slower cooling of cells 3 mm or more from the surface may result in cellular dehydration. Such information can be used for pretreatment planning and optimization of LN_2 spray cryosurgical protocols of skin and eventually, other organs.

6. Nomenclature

a	radial distance of isotherm, m
b	axial distance of isotherm, m
C	specific heat, J/kg K
h	heat transfer coefficient, W/m^2 K
k	thermal conductivity, W/m K
L	latent heat, J/kg
m	regression constant,
n	regression constant,
Q	heat generation, W/m^3
R_0	radius of cooling site, m
r	radial coordinate, m

T	temperature, K, ºC
t	time, s
z	axial coordinate, m

Greek

α	thermal diffusivity, m^2/s
λ	root of transcendental function
ρ	mass density, kg/m^3
θ	angular coordinate
τ	dimensionless time

Subscript

a	air
b	blood
f	frozen
i	initial
l	liquid
m	melting, metabolism
$m1$	liquidus
$m2$	solidus
s	solid
u	unfrozen

7. References

1. T.E. Cooper and W.K. Petrovic, An Experimental Investigation of the Temperature Field Produced by a Cryosurgical Cannula, Journal of Heat Transfer, vol. 96, pp. 415-420, 1974.
2. B. Rubinsky, Cryosurgery, Annual Review of Biomedical Engineering, vol. 2, pp. 157-187, 2000.
3. S.A. Zacarian, Cryosurgery of Tumors of the Skin and Oral Cavity, Charles C Thomas, Illinois, 1973.
4. D. Torre, Cutaneous Cryosurgery, Journal of Cryosurgery, vol. 1, pp. 202-209, 1968.
5. M.D. Andrews, Cryosurgery for Common Skin Conditions, American Family Physician, vol. 69, pp. 2365-2372, 2004.
6. T.E. Cooper and G.J. Trezek, On the Freezing of Tissue, Journal of Heat Transfer, vol. 94, pp. 251-253, 1972.
7. T.E. Cooper and G.J. Trezek, Rate of Lesion Growth around Spherical and Cylindrical Cryoprobes, Cryobiology, vol. 7, pp. 183-190, 1971.
8. G.J. Trezek, Heat Transfer in Medicine and Biolody: Analysis and Applications, Plenum Press, New York, 1985.
9. G. Comini and S.D. Giudice, Thermal Aspects of Cryosurgery, Journal of Heat Transfer, vol. 98, pp. 543-549, 1976.
10. B. Rubinsky and A. Shitzer, Analysis of a Stefan-like problem in a Biological Tissue around a Cryosurgical Probe, Journal of Heat Transfer, vol. 98, pp. 514-519, 1976.
11. Y. Rabin and A. Shitzer, Exact Solution to the One-Dimentioanl Inverse-Stephan Problem in Nonideal Biological Tissues, Journal of Heat Transfer, vol. 117, pp. 425-431, 1995.
12. Y. Rabin and A. Shitzer, Numerical Solution of the Multidimentional Freezing Problem during Cryosurgery, Journal of Biomedical Engineering, vol. 120, pp. 32-37, 1998.
13. R.G. Keanini and B. Rubinsky, Optimization of Multiprob Cryosurgery, Journal of Heat Transfer, vol. 114, pp. 796-801, 1992.
14. H. Budman, A. Shitzer and J. Dayan, Analysis of the Inverse Problem of Freezing and Thawing of a Binary Solution during Cryosurgical Processes, Journal of Biomedical Engineering, vo. 117, pp. 193-202, 1995.
15. J.S. Hong, S. Wong, G. Pease, and B. Rubinsky, MR Imaging Assisted Temperature Calculations during Cryosurgery, Magn. Reson. Imaging, vol. 12, pp. 1021-1031, 1994.
16. A. Weill, A. Shitzer, and P. Bar-Yoseph, Finite Element Analysis of the Temperature Field around Two Adjacent Cryoprobes, Journal of Biomedical Engineering, vol. 115, pp. 374-378, 1993.
17. R. Wan, Z. Liu, K. Muldrew and J. Rewcastle, A Finite Element Model for Ice Ball Evolution in a Muti-Probe Cryosurgery, Computer Methods in Biomechanics and Biomedical Engineering, vol. 6, pp. 197-208, 2003.
18. J. Rewcastle et al, A Model for the Time-Dependent Thermal Distribution within an Iceball Surrounding a Cryoprobe, Phys. Med. Biol., vol. 43, pp. 3519-3534, 1998.
19. N.E. Hoffmann and J.C. Bischof, Cryosurgery of Normal and Tumor Tissue in the Dorsal Skin Flap Chamber: Part I - Thernal Responses, Journal of Biomedical Engineering, vol.123, pp. 301-309, 2001.
20. I.S. Cooper, Engineering in the Practice of Medicine, Williams & Wilkins, Baltimore, 1967.
21. W. Franco, J. Liu, G.-X. Wang, J.S. Nelson and G. Aguilar, Radial and Temporal Variations in Surface Heat Transfer during Cryogen Spray Cooling, Physics in Medicine and Biology, vol. 50, pp. 387-397, 2005.
22. M.N. Ozisik, Heat Conduction (2nd Edition), John Wiley & Sons, New York, 1993.
23. D.J. Smith, R.V. Devireddy, J.C. Bischof, Prediction of thernal history and interface propagation during freezing in biological systems - Latent heat and temperature-Dependent property Effects, Proc. 54th ASME/JSME Joint Thermal Engineering Conference, San Diego, CA, 1999.
24. F.A. Duck, Physical Properties of Tissue, Academic Press, San Diego, 1990.
25. A.Alexiades and A.D. Solomon, Mathmatical Modeling of Melting and Freezing Processes, Hemisphere, Washington D.C., 1993.
26. G. Aguilar, G.-X. Wang and J.S. Nelson, Effect of Spurt Duration on the Heat Transfer Dynamics during Cryogen Spray Cooling, Physics in Medicine and Biology, vol. 48, pp. 2169-2181, 2003.
27. W.H. Yang, H.H. Peng, H.C. Chang, et al, An in vitro monitoring system for simulated thermal process in cryosurgery, Cryobiology, vol. 40, pp.

159-170, 2000.
28. N.E. Hoffmann and J.C. Bischof, The Cryobiology of Cryosurgical Injury, Urology (Supplement 2A), vol. 60, pp. 40-49, 2002.
29. A.A. Gage, J. A. Caruana, M. Montes, Critical Temperature for Skin Necrosis in Experiment Cryosurgery, Cryobiology, vol. 19, pp. 273-282, 1982.
30. Committee on Guidelines of Care, Guidelines of care for cryosurgery, Journal of the American Academy of Dermatology, vol. 31, pp. 648-653, 1994.
31. E.G. Kuflik, Cryosurgery updated, Journal of the American Academy of Dermatology, vol. 31, pp. 925-944, 1994.
32. X. He, J.C. Bischof, Quantification of Temperature and Injury Response in Thermal Therapy and Cryosurgery, Critical Review in Biomedical Engineering, vol. 31, pp. 355-421, 2003.
33. P. Mazur and C. Koshimoto, Is Intracellular Ice Formation the Cause of Death of Mouse Sperm Frozen at High Cooling Rate? Biology of Reproduction, vol. 66, pp. 1485-1490, 2002.